Contract # N00014-14-C-0004

Autonomous Control Modes and Optimized Path Guidance for Shipboard Landing in High Sea States

Progress Report (CDRL A002)

Progress Report for Period: January 10, 2017 to April 9, 2017

PI: Joseph F. Horn 814-865-6434 joehorn@psu.edu Junfeng Yang Grad. Research Assistant Penn State University	Co-PI: Chengjian He (408) 523-5100 he@flightlab.com Dooyong Lee Advanced Rotorcraft Technologies	Co-PI: Sean Roark (301)995-7093 sean.roark@navy.mil Geraldo Gonzalez NAVAIR 4.3.2.4 John Tritschler U.S. Navy Test Pilot School

Performing Organization:
The Pennsylvania State University
Department of Aerospace Engineering
231C Hammond Building
University Park, PA 16802
Attn: Joseph F. Horn
Phone: 814-865-6434, Fax: 814-865-7092
Email: joehorn@psu.edu

Prepared under:
Contract Number N00014-14-C-0004
2012 Basic and Applied Research in Sea-Based Aviation
ONR #BAA12-SN-028
CDRL A002

Report Distribution per CDRLs for Contract No. N00014-14-C-0004

ENCLOSURE NUMBER 1
CONTRACT DATA REQUIREMENTS LIST
INSTRUCTIONS FOR DISTRIBUTION

DISTRIBUTION OF TECHNICAL REPORTS, FINAL REPORT, THEORY AND USER MANUAL FOR SOFTWARE
(A SF 298 must accompany the final report)

		NUMBER OF COPIES	
ADDRESSEE	**DODAAC CODE**	**UNCLASSIFIED / UNLIMITED**	**UNCLASSIFIED/ LIMITED AND CLASSIFIED**
COR: Mr. John Kinzer ONR Code 351 E-Mail: john.kinzer@navy.mil	N00014	1	1
Program Officer: Dr. Judah Milgram ONR Code 351 E-Mail: judah.milgram@navy.mil	N00014	1	1
Program Officer: Ms. Susan Polsky NAVAIR 4.3.2.1 E-Mail: susan.polsky@navy.mil	N00024		
Administrative Contracting Officer* E-Mail: onr_chicago@onr.navy.mil	N62880	1	1
Director, Naval Research Lab Attn: Code 5596 4555 Overlook Avenue, SW Washington, D.C. 20375-5320 E-mail: reports@library.nrl.navy.mil	N00173	1	1
Defense Technical Information Center 8725 John J. Kingman Road STE 0944 Ft. Belvoir, VA 22060-6218 E-mail: tr@dtic.mil	HJ4701	1	1

* Send only a copy of the transmittal letter to the Administrative Contracting Officer; do not send actual reports to the Administrative Contracting Officer.

ELECTRONIC SUBMISSIONS OF TECHNICAL REPORTS IS PREFERRED AND ENCOURAGED. ELECTRONIC SUBMISSION SHOULD BE SENT TO THE E-MAIL ADDRESSES PROVIDED IN THE ABOVE TABLE, HOWEVER PLEASE NOTE THE FOLLOWING:

- Only Unlimited/Unclassified document copies may be submitted by e-mail.
- Unclassified/Limited has restricted distribution and a classified document (whether in its entirety or partially) is to be distributed in accordance with classified material handling procedures.
- Electronic submission to DIRECTOR, NAVAL RESEARCH LAB, shall be unclassified/unlimited reports and 30 pages or less. If unclassified and more than 30 pages,

Section I: Project Summary

1. Overview of Project

This project is performed under the Office of Naval Research program on Basic and Applied Research in Sea-Based Aviation (ONR BAA12-SN-0028). This project addresses the Sea Based Aviation (SBA) initiative in Advanced Handling Qualities for Rotorcraft.

Landing a rotorcraft on a moving ship deck and under the influence of the unsteady ship airwake is extremely challenging. In high sea states, gusty conditions, and a degraded visual environment, workload during the landing task begins to approach the limits of a human pilot's capability. It is a similarly demanding task for shipboard launch and recovery of a VTOL UAV. There is a clear need for additional levels of stability and control augmentation and, ultimately, fully autonomous landing (possibly with manual pilot control as a back-up mode for piloted flight). There is also a clear need for advanced flight controls to expand the operational conditions in which safe landings for both manned and unmanned rotorcraft can be performed. For piloted rotorcraft, the current piloting strategies do not even make use of the available couplers and autopilot systems during landing operations. One of the reasons is that, as the deck pitches and rolls in high sea states, the pilot must maneuver aggressively to perform a station-keeping task over the landing spot. The required maneuvering can easily saturate an autopilot that uses a rate limited trim system. For fly-by-wire aircraft, there is evidence that the pilot would simply over-compensate and negate the effectiveness of a translation rate command/position hold control mode. In addition, the pilots can easily over-torque the rotorcraft, especially if they attempt to match the vertical motion of the deck.

This project seeks to develop advanced control law frameworks and design methodologies to provide autonomous landing (or, alternatively, a high level of control augmentation for pilot-in-the-loop landings). The design framework will focus on some of the most critical components of autonomous landing control laws with the objective of improving safety and expanding the operational capability of manned and unmanned rotorcraft. The key components include approach path planning that allows for a maneuvering ship, high performance station-keeping and gust rejection over a landing deck in high winds/sea states, and deck motion feedback algorithms to allow for improved tracking of the desired landing position and timing of final descent.

2. Activities this period

Task 11–Optimization of Control Parameters

Techniques for gain tuning of Dynamic Inversion (DI) control law and auxiliary concepts have been developed in this progress period. As in DI controller the trajectory tracking algorithm is realized in an inner-outer loop scheme, where multiple PID gains need to be selected in an optimal sense. In the preceding work, those PID gains were set with empirical values, which seem satisfactory in terms tracking performance, but the effort of last period proposed a systematic method to evaluate the "optimality" of control parameters from a wider perspective, and also provided a way to find out the optimal parameters.

As has been revealed in the theory part of DI controller, the PID gains governs the error dynamics of output variable,

$$\dot{e}_y = \dot{y}_r - \dot{y} = -G \tag{1}$$

where G is the output of PID compensator used in the DI controller, the gains should be designed in such a way that the output error decays with desirable properties, i.e. quickly, smoothly and with little

steady-state residual. The error decaying properties have explicit linkage with PID gains, e.g. the pitch and roll attitude use PID compensator including attitude rate, attitude angle, and integral of attitude angle generally formulated in Equ.(2)

$$G = K_p e_y + K_i \int e_y dt + K_{ii} \iint e_y dt^2 \tag{2}$$

This PID compensator specifies a 3rd order error dynamics which can be factorized as follow:

$$\left(s^2 + 2\zeta_e \omega_e s + \omega_e^2\right)\left(s + p_e\right) = 0 \tag{3}$$

There is an explicit relation between error decaying properties and PID gains expressed in Equ.(4):

$$\begin{aligned} K_p &= 2\zeta_e \omega_e + p_e \\ K_i &= 2\zeta_e \omega_e p_e + \omega_e^2 \\ K_{ii} &= \omega_e^2 p_e \end{aligned} \tag{4}$$

Eqn. (4) implies that design PID gains is equivalent to designing the error decaying parameters, however the later have more clear physical significance, namely, ω_e governs error decaying quickness, ζ_e governs the overshooting during transient, and p_e determines the steady state error. The outer loop control laws are also designed using DI, where the input of the dynamics model is the inner loop command signal. A very simplified dynamic model is usually used in the outer loop design, for longitudinal, lateral position control Eq.(5) provides adequate fidelity.

$$\begin{aligned} \dot{V}_x^{HHF} &\approx -g \cdot \theta \\ \dot{V}_y^{HHF} &\approx g \cdot \phi \end{aligned} \tag{5}$$

The DI control law yields:

$$\theta_{cmd} = -\frac{1}{g}\left(K_{p_{Xlon}}\left(X_{ref}^{HHF} - X^{HHF}\right) + K_{i_{Xlon}} \int \left(X_{ref}^{HHF} - X^{HHF}\right) dt + K_{p_{Vlon}}\left(V_{Xref}^{HHF} - V_X^{HHF}\right) + \frac{dV_{Xref}^{HHF}}{dt} \right) \tag{6}$$

$$\phi_{cmd} = \frac{1}{g}\left(K_{p_{Ylat}}\left(Y_{ref}^{HHF} - Y^{HHF}\right) + K_{i_{Ylat}} \int \left(Y_{ref}^{HHF} - Y^{HHF}\right) dt + K_{p_{Vlat}}\left(V_{Yref}^{HHF} - V_Y^{HHF}\right) + \frac{dV_{Yref}^{HHF}}{dt} \right) \tag{7}$$

There are multiple PID gains in the inner and outer loop controller, to reduce the DOF of to be determined parameters, following empirical assumptions are imposed, the integrator poles are located at 1/5 of natural frequency of error dynamics, damping ratio of error dynamics takes critical value, the ratio of natural frequency of outer-loop to inner-loop's is set to be 1/5 to facilitate frequency separation. Under those assumptions, the longitudinal group of PID gains depends on the frequency parameter of pitch error dynamics $\omega_{e\theta}$, similarly the lateral group of PID gains depends on the frequency parameter of roll error dynamics $\omega_{e\phi}$. In Ref.1 the controller gain tuning is framed as a design trade-off between high gain designs for disturbance rejection versus lower gain design for more robust stability of the closed loop system. The gain tuning of PID compensator of DI control law follows the same reasoning. The behind philosophy is when the frequency parameter increases, the PID compensator has higher gain thus better tracking performance, in the other case, when the frequency parameter decreases , the close-loop system will have less risk of raising a control system induced instability.

The tracking performance and close-loop robust stability are quantified by Disturbance Rejection Bandwidth (DRB) and Gain Margin/Phase Margin of loop-breaking system. The calculation of DRB and GM/PM are based on a high order linear model of rotorcraft, actuator and controller. The schematic was illustrated in Figure 1.

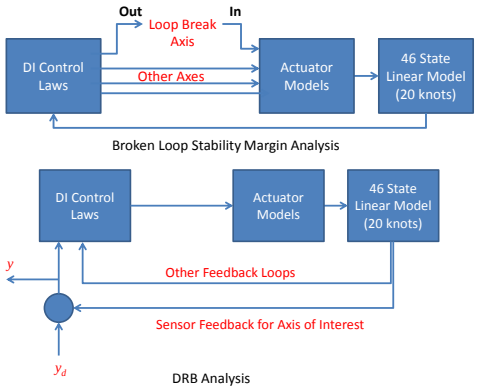

Figure 1. Schematics of Linear Model for DRB & SM Analysis

The GM/PM are transfer function defined concept, for each of the pitch/roll/yaw/heave axes a loop-breaking transfer function can be obtained, thus each axis has its GM, PM. The loop-breaking transfer function is obtained by disconnecting the actuator of the axis of interest, while keeping all other loops connected. DRB analysis looks at the frequency response of the "disturbance in" to "disturbance out" transfer function $\frac{y}{y_d}(s)$. DRB is defined as the maximum frequency with magnitude less than -3 dB, and represents the maximum frequency disturbance that can be rejected for a particular controlled variable. For the shipboard recovery task, autonomous full trajectory control is considered, so the position hold (the outer most loop) is analyzed. For the present study, the focus is on the lateral and longitudinal axis control only. Figures 2-5 demonstrate the stability margin analysis and disturbance rejection analysis of a medium gain design corresponding $\omega_{e\phi} = 2.5$ rad/sec, $\omega_{e\theta} = 2.5$ rad/sec. Note that both axes exhibit phase crossovers at both low and high frequencies. The open loop dynamics of the helicopter are unstable in low speed flight, so there is a minimum gain to stabilize the helicopter. The more critical gain margin is based on the high frequency crossover, which results in an upper gain limit to avoid instability due to rotor-body coupling.

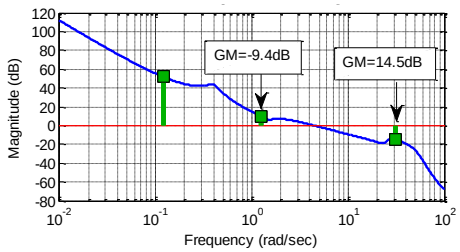

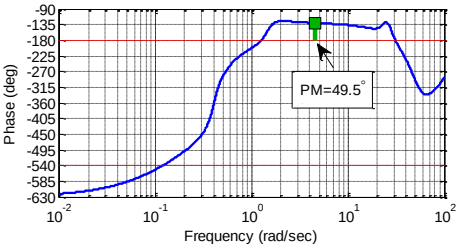

Figure 2. Stability Margin of Pitch Axis

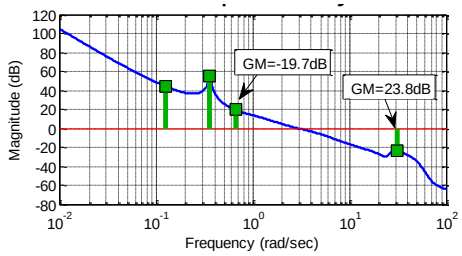

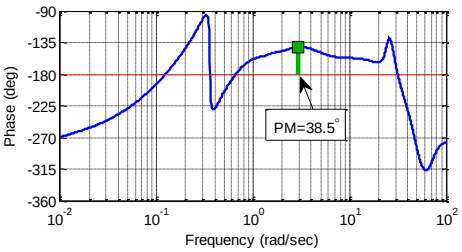

Figure 3. Stability Margin of Roll Axis

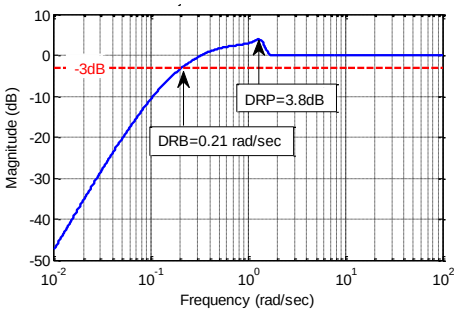

Figure 4. Disturbance Rejection Analysis for Longitudinal Position Hold

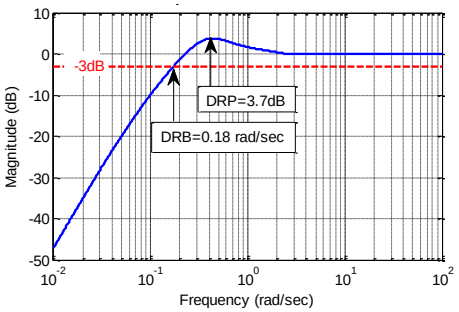

Figure 5. Disturbance Rejection Analysis for Lateral Position Hold

The variations of SM and DRB with increasing frequency parameter $\omega_{e\theta}$ or $\omega_{e\phi}$ were investigated by sweeping each parameter from 1.5 to 4.0 rad/sec while the other parameter is held constant. Table 1 summarizes the analysis results for the lateral axis. Disturbance rejection in lateral and longitudinal position hold was analyzed in addition to stability margins in the other axes. Since the core of the DI control law effectively de-couples the dynamics, the other axes are practically unaffected by the roll-axis parameter variation. The lateral axis DRB clearly increases monotonically with the increasing parameter, showing the expected improvement in performance with higher gain, while performance and stability in other axes are unchanged. The lateral axis stability margins vary slightly for small values, but for larger values the phase margins starts to decrease until dropping below 30° for the highest value. There is a corresponding increase in Disturbance Rejection Peak for high gain. The degradation in stability is due to the interaction of higher order dynamics with higher gain. Eventually, for very high gain, rotor-body coupling effects and instability can be observed. The trade-off between PM and DRB can be clearly observed in Figure 6. Similar analysis was performed on longitudinal axis with its results summarized in Table 2 and Figure 7.

Table 1. Variation in Lateral Axis Gain

Roll / Pitch Frequency Parameters		**Disturbance Rejection in Y Position**		**Disturbance Rejection in X Position**		**Lat. Axis Stability Margins**		**Long. Axis Stability Margins**		**Heave Axis Stability Margins**		**Yaw Axis Stability Margins**	
$\omega_{e\phi}$ **(rad/s)**	$\omega_{e\theta}$ (rad/s)	DRB (rad/s)	DRP (dB)	DRB (rad/s)	DRP (dB)	PM (deg)	GM (dB)	PM (deg)	GM (dB)	PM (deg)	GM (dB)	PM (deg)	GM (dB)
1.5	2.5	0.11	3.2	0.21	3.9	35.5	+8.9 -23.0	49.9	+14.8 -9.0	51.2	+29.0 -21.8	74.0	+∞ -16
2.0	2.5	0.14	3.5	0.21	3.9	38.3	+19.1 -19.0	49.7	+14.7 -9.4	51.3	+29.0 -21.8	73.8	+∞ -17
2.5	2.5	0.17	3.7	0.21	3.9	38.5	+23.8 -19.7	49.5	+14.5 -9.4	51.3	+29.0 -21.8	73.9	+∞ -17
3.0	2.5	0.20	4.0	0.21	3.9	35.8	+19.3 -21.0	49.4	+14.2 -9.3	51.2	+29.0 -21.8	74.5	+∞ -17
3.5	2.5	0.23	4.3	0.21	3.9	31.4	+16.3 -19.1	49.4	+14.0 -9.3	51.2	+29.0 -21.8	75.8	+∞ -16
4.0	2.5	0.26	4.6	0.21	3.9	27.2	+14.0 -18.0	49.6	+13.8 -9.3	51.1	+29.1 -21.8	77.6	+∞ -16

Table 2. Variation in Longitudinal Axis Gain

Roll / Pitch Frequency Parameters		**Disturbance Rejection in Y Position**		**Disturbance Rejection in X Position**		**Lat. Axis Stability Margins**		**Long. Axis Stability Margins**		**Heave Axis Stability Margins**		**Yaw Axis Stability Margins**	
$\omega_{e\phi}$ **(rad/s)**	$\omega_{e\theta}$ (rad/s)	DRB (rad/s)	DRP (dB)	DRB (rad/s)	DRP (dB)	PM (deg)	GM (dB)	PM (deg)	GM (dB)	PM (deg)	GM (dB)	PM (deg)	GM (dB)
2.5	**1.5**	0.17	3.8	0.13	2.9	38.4	+24.3 -18.8	67.4	+20.7 -11.7	52.4	+28.1 -22.4	73.8	+∞ -14
2.5	**2.0**	0.17	3.7	0.17	3.3	38.4	+24.1 -19.6	56.6	+17.1 -10.9	51.8	+28.6 -21.9	73.8	+∞ -14
2.5	**2.5**	0.17	3.7	0.21	3.9	38.5	+23.8 -19.7	49.5	+14.5 -9.4	51.3	+29.0 -21.8	73.9	+∞ -17
2.5	**3.0**	0.17	3.7	0.25	4.4	38.3	+23.3 -19.6	44.4	+12.3 -8.7	51.0	+29.5 -21.8	74.0	+∞ -18
2.5	**3.5**	0.17	3.7	0.29	4.7	38.0	+22.8 -19.5	40.4	+10.4 -8.9	51.0	+30.1 -21.8	74.2	+∞ -18
2.5	**4.0**	0.17	3.6	0.33	4.8	37.4	+22.1 -19.4	37.1	+8.9 -9.9	51.0	+30.7 -21.8	74.3	+∞ -18

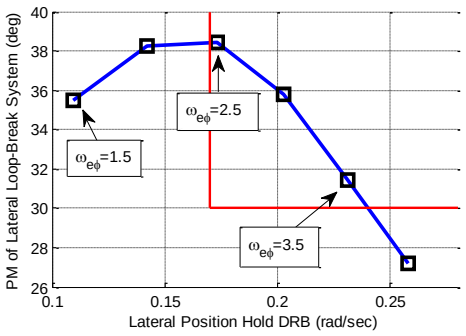

Figure 6. Phase Margin vs. Position Hold DRB of Lateral Axis

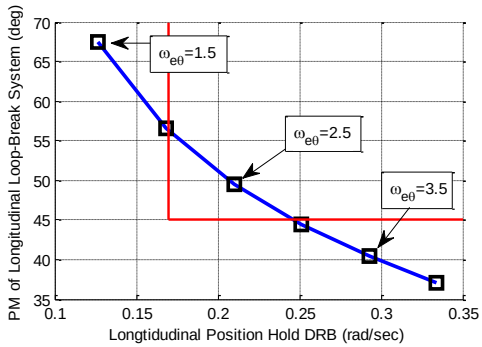

Figure 7. Phase Margin vs. Position Hold DRB of Longitudinal Axis

Figure 6-7 imply that a reasonable compromise between SM and DRB can be achieved by specifying $\omega_{e\phi} = 3.0$ rad/sec, $\omega_{e\theta} = 2.5$ rad/sec, the corresponding gain set will be the nominal design. Non-linear simulations were used to validate the nominal gains, and also to prove the impact of low/high gains on tracking error and stability margin. The test-bed is a medium class simulation model station-keeping over a moving destroyer deck with 20 knots forward speed. The deck motion is based on the SCONE ship motion dataset, airwake fidelity is provided by CFD solutions of the SFS2 frigate shape in 20 knots headwinds. In the test scenario, the helicopter starts at 1000 ft behind flight deck, with an initial speed of 60 ft/sec, throughout the simulation the helicopter approaches to flight deck, and then keeps hovering over flight deck tracking the center of the deck. The initial settings of the simulation are shown in Figure 8.

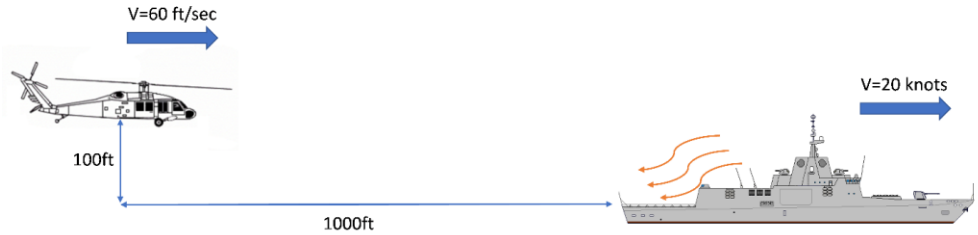

Figure 8. Initial Setting of Simulation

Analysis of the simulation results will focus on the lateral axis. The lateral axis presents a more challenging tracking problem due to the rolling motion of the ship deck (as the helicopter performs station-keeping over the center of the deck), and the lower inertia in the roll axis resulting in larger airwake disturbances. As indicated in Table 3, multiple simulations were performed with $\omega_{e\phi}$ sweeping from 1.5 rad/sec to 4.0 rad/sec while $\omega_{e\theta}$ was held at its nominal value 2.5 rad/sec, metrics used to characterize disturbance rejection properties are RMS of longitudinal and lateral tracking error. Analysis of control actuation focused on the high frequency activity of the longitudinal and lateral cyclic. The "high frequency shooting" of the cyclic pitch is defined as the difference between the actuator travel and a smoothed version of the signal. The smoothed signal is obtained by applying a non-causal low-pass FIR digital filter to the original data. The FIR filter has to meet certain specifications such as pass-band, transition width, and stop band attenuation. The typical frequency of swashplate actuation suggests that pass band of 3 Hz, transition width of 0.3375 Hz, stop band attenuation of -54dB are desirable for smoothing operation. A FIR filter formulated in Eq. (8) using 1001 data points can meet all the requirements.

$$y[n] = \sum_{k=-500}^{500} x[n+k]h[k] \quad (8)$$

Where $h[k] = \frac{\sin(0.01k)}{\pi k}\left(0.54 + 0.46\, cos\left(\frac{2\pi k}{1001}\right)\right)$

Figure 9 demonstrates the separation of high frequency shooting from lateral cyclic pitch. An RMS of the high frequency signal can then be used to assess the unfavorable actuator activity of the controller.

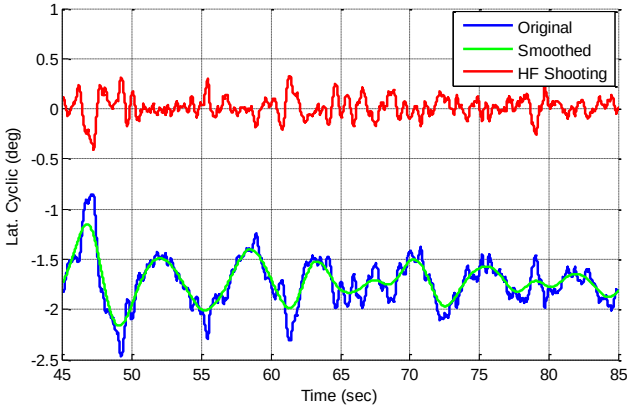

Figure 9. Separation of High Frequency Shooting

Table 3. Summary of Performance with Sweep of Roll Axis Frequency Parameter

$\omega_{e\phi}$ (rad/sec)	$\omega_{e\theta}$ (rad/sec)	RMS of X_e(ft)	RMS of Y_e(ft)	RMS of θ_{1s} (deg)	RMS of θ_{1c} (deg)
1.5	2.5	1.01	2.05	0.1662	0.0516
2.0	2.5	0.99	0.96	0.1662	0.0630
2.5	2.5	1.01	0.39	0.1662	0.0802
3.0	2.5	1.03	0.26	0.1662	0.1146
3.5	2.5	1.03	0.20	0.1604	0.1375
4.0	2.5	1.04	0.16	0.1604	0.1662

Figure 10-12 juxtapose the lateral tracking performance, lateral fuselage rate and lateral cyclic pitch for three cases with $\omega_{e\phi}$=1.5 rad, $\omega_{e\phi}$=3.0 rad/sec, $\omega_{e\phi}$=4.0 rad/sec, they represent a low gain design, nominal design and high gain design respectively. Those figures reveal that reducing controller gains leads to poor tracking performance indicated by the large amplitude waves of green line in Figure 10; while increasing controller gains certainly improves the tracking tightness but at the cost of tightened coupling of rotor dynamics and fuselage dynamics, the latter is characterized by the high frequency shooting in fuselage rate and cyclic pitch of swashplate. A test of an extremely high gain design of $\omega_{e\phi}$=7.5 basically pushes the rotorcraft to the edge of instability, expressed as air-resonance in Figure 13.

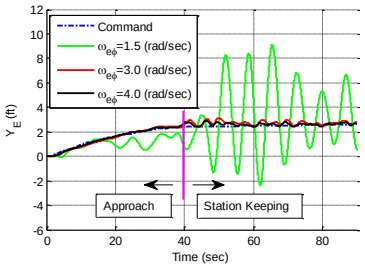

Figure 10. Lateral Tracking Performance

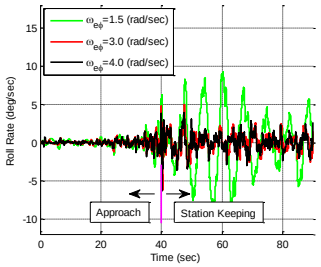

Figure 11. Roll Rate Response

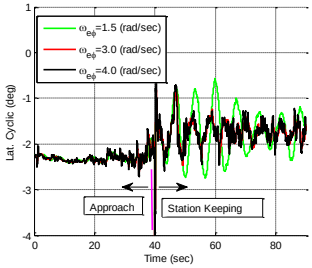

Figure 12. Lateral Cyclic Pitch

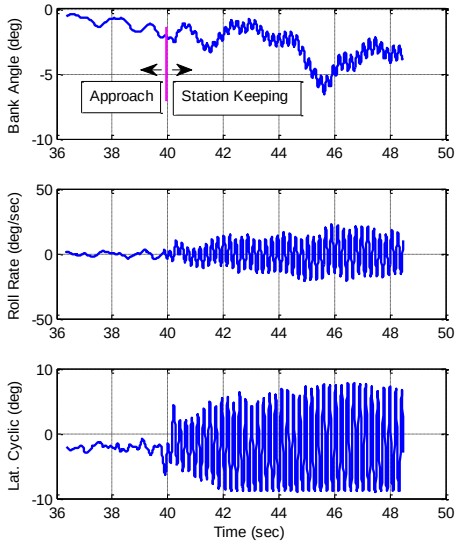

Figure 13. Example of extremely high controller gains - air resonance

Traditionally, both industry and regulatory documents use loop-breaking GM/PM as the metrics for robust stability. In fact, axis-wise GM/PM are optimistic estimations of the robust stability of MIMO systems, since loop-break should be performed in each loop and everywhere to ensure that any disturbance is not amplified in the loop, even this is not adequately saying the close-loop system of full order model can withstand the most adverse combination of all possible disturbance. The robust control theory on the other hand provides a MIMO perspective for the stability, where the MIMO stability criteria provides a conservative estimation of the close-loop stability, this is an absolute stability even in the worst case. The robustness of a MIMO controller is all about its capability of stable working when it is design on a reduced order model G_r, while implemented to a full order model G_f. The difference between reduced and full order model is the modeling error ΔG . In rotorcraft control practice, the modeling error primarily stems from the unmodeled dynamics, e.g. when generating the reduced order model, it is common to ignore flap/lag dynamics, actuator dynamics and sensor dynamics. This type of modeling error can be extracted by Eq. (9)

$$\Delta\bar{G} = \bar{G}_f(\bar{G}_r)^{-1} - I \tag{9}$$

Robust control theory [3][4] asserts that once we specify a design model G_r , and accept the existence of unstructured modeling error in the form Eq.(9), the feedback controller in Figure.14 would work stably with G_f , if

1. The nominal feedback close-loop system $G_r(s)K(s)[I + G_r(s)K(s)]^{-1}$ is stable
2. The perturbed system $G_f(s)$ and the nominal system $G_r(s)$ have the same number of unstable poles.
3. Condition $\underline{\sigma}[I + (G_rK)^{-1}] > \overline{\sigma}(\Delta G)$ is satisfied

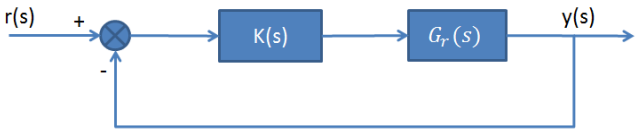

Figure 14. The Negative Feedback System of Nominal Model

In the current study, reduced order model used for DI controller design has 8 state variables $x_r = [\phi \quad \theta \quad u \quad v \quad w \quad p \quad q \quad r]$, full order model has 46 state variables, the poles of both models are plotted in Figure 15-16 respectively, it is noteworthy that both model have the same number of unstable poles, which is a prerequisite to apply the robustness criteria.

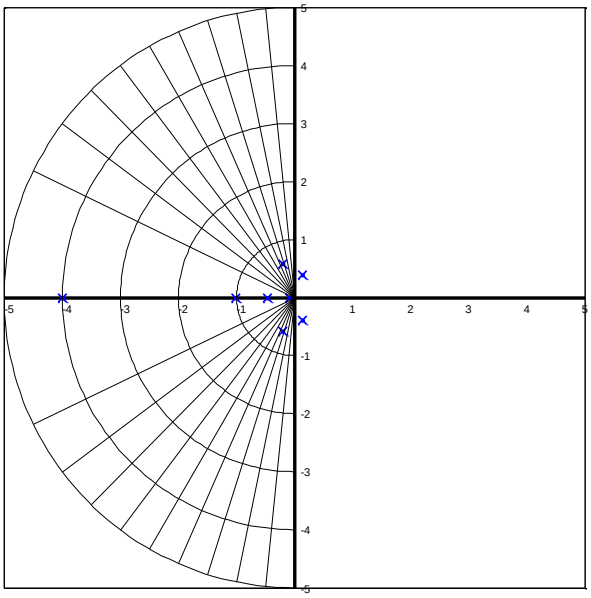

Figure 15. Poles of Reduced Order model

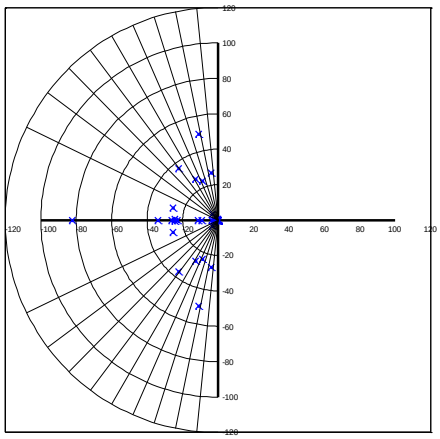

Figure 16.a Poles of Full Order Model

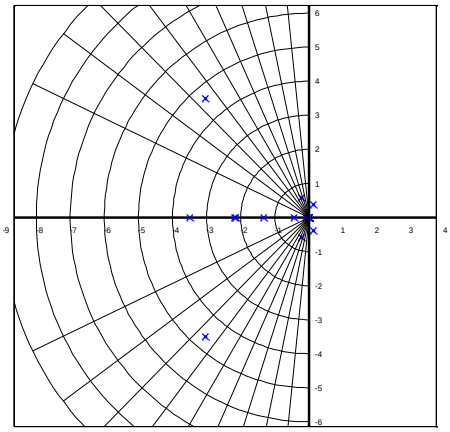

Figure 16.b Poles of Full Order Model (Zoom In)

The output vector of each model is defined as: $y=\begin{bmatrix} w & p & q & r \end{bmatrix}$. The transfer function matrix G_r and G_f can then be extracted from the state space model, and the modeling error also can be acquired following Eq.(9) , Figure 17-18 illustrate the singular value of reduced order, full order model and modeling error. Note that the singular value plot of modeling error has two branches of large value in the low frequency range, which means the modeling error is not applicable, however the low frequency range is usually not the origin of trouble, thus we will just ignore this frequency band.

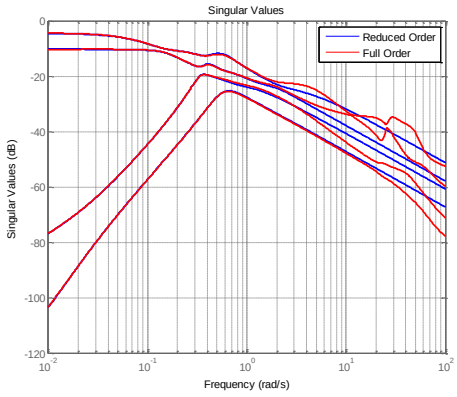

Figure 17. Comparison of the Singular Value of $G_r(s)$ and $G_f(s)$

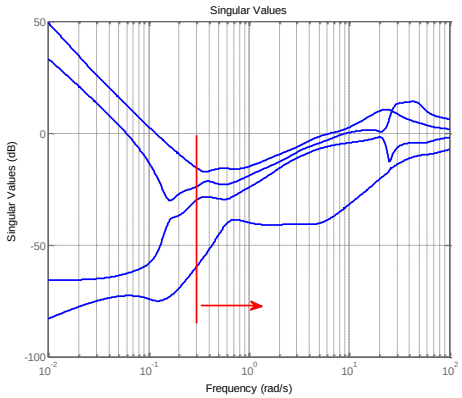

Figure 18. Singular Value of Multiplicative Modeling Error

Since the robust control theory supports only an output-based controller, while DI controller needs feedback of multiple states, namely $u,v,\phi,\theta,u,v,X_{lon},Y_{lat},H$, necessarily the parameter estimation is used to reconstruct the

controller. The non-output variables can be estimated by reliable linear relations as follow

$$\frac{d\phi}{dt} = p + q\sin\phi_{trim}\tan\theta_{trim} + r\cos\phi_{trim}\tan\theta_{trim}$$
$$\frac{d\theta}{dt} = q\cos\phi_{trim} - r\sin\phi_{trim}$$
$$\frac{d\psi}{dt} = q\frac{\sin\phi_{trim}}{\cos\theta_{trim}} + r\frac{\cos\phi_{trim}}{\cos\theta_{trim}}$$
$$\frac{du}{dt} \approx X_u \cdot u - g\theta + X_q \cdot q$$
$$\frac{dv}{dt} \approx Y_v \cdot v + g\phi + Y_p \cdot p$$
$$\frac{dX_{lon}}{dt} \approx u$$
$$\frac{dY_{lat}}{dt} = v$$

The trim attitude angle and stability derivatives come from trim result and reduced order linear model. After preparing the controller and modeling error, the robustness criteria $\underline{\sigma}[I + (\bar{G}_r K)^{-1}] > \overline{\sigma}(\Delta\bar{G})$ can be evaluated, a range of gain setting were investigated to demonstrate the relation between robustness and increasing gains. Three pairs have been researched, namely $\left[\omega_{n\phi}, \omega_{n\theta}\right]$ = [2,2], [3,3] and [4,4], the robustness criterion were plotted in Figure 19, the plot implies that as tracking performance gets more emphasized by applying higher gain, the robustness margin reduces, to some level when the controller minimum singular value intersects modeling error singular value, the robustness is no more ensured.

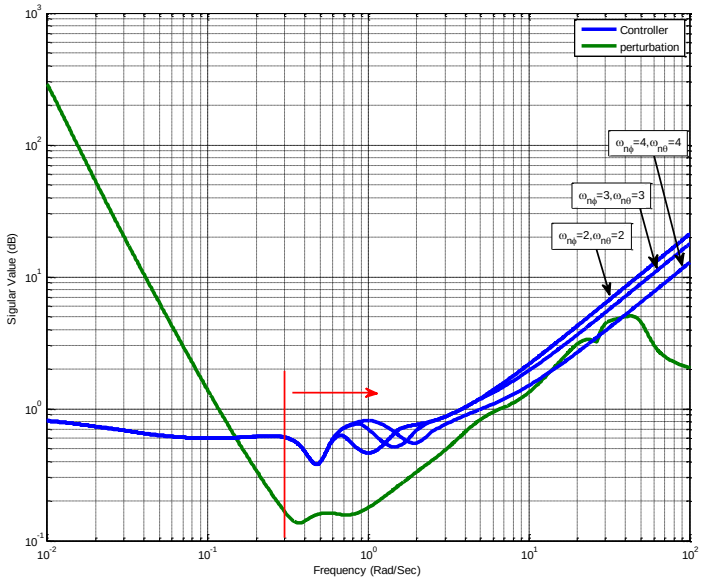

Figure 9. Robustness Criterion for Different Gain Setting

3. Significance of Results

1) A systematic method of PID gain tuning for DI controller is developed, this is essentially a frequency-domain method and treats the optimization as a tradeoff between SM and DRB. SISO based loop-breaking techniques were developed to accommodate the calculation of SM and DRB. This method is particularly straightforward in terms of compliance with ADS-33 and other regulatory criteria (Ref. 1), and non-linear simulations proved the effectiveness of the approach. The results also showed that in the context of DI, the SISO methodologies are effective as the feedback linearization scheme effectively decouples the different axes. Parameters in a single axis show the desired performance stability tradeoff while the other axes are largely unaffected. The approach does require manual tuning and independent design of each axis.
2) A MIMO robust stability criteria was applied to DI controller and rotorcraft, this criteria shows consistent with SISO solution stability margin variation with increasing gains, theoretically it can be used to guide controller design, or used to supplement defining the stability margin. Due to the fact that very few regulatory documents involve MIMO stability criteria, the quantity of robust stability margin need to be established to facilitate its application.

4. Plans and upcoming events for next reporting period

Prototype development and evaluation: The next phase of the work will begin rigorous testing and evaluations of the controllers. This includes batch simulations and piloted simulation studies.

5. References

1. Mansur, M. H., Lusardi, J. A., Tischler, M. B., and Berger, T., "Achieving the Best Compromise between Stability Margins and Disturbance Rejection Performance," American Helicopter Society 65th Annual Forum Proceedings, Grapevine, TX, May, 2009.
2. Joseph F. Horn, Junfeng Yang, Dooyong Lee, Cheengjian He, "Parameter Optimization of Dynamic Inversion Control Laws for Shipboard Operations," American Helicopter Society 73th Annual Forum Proceedings, Fort Worth, Texas, May, 2017.
3. John C. Doyle and Gunter Stein., "Multivariable Feedback Design: Concepts for a Classical/Modern Synthesis," IEEE Transaction on Automatic Control, Vol.AC-26, No.1, February 1981
4. Alok Sinha, "Linear Systems Optimal and Robust Control," CRC press, 2007

6. Transitions/Impact

Submitted AHS Forum Paper and presented paper at AHS UAV Specialist meeting.

7. Collaborations

Penn State and ART have collaborated directly with John Tritschler and Sean Roark at NAVAIR. In addition, we are communicating with other Navy researchers pursuing similar projects: Al Schwarz at NSWCCD and Dave Findlay at NAVAIR.

8. Personnel supported

Principal investigator: Joseph F. Horn

Graduate Students: Junfeng Yang, PhD Candidate

9. Publications

1. Horn, J. F., Yang, J., He, C., and Lee, D., "Parameter Optimization of Dynamic Inversion Control Law for Shipboard Operations," *American Helicopter Society 73th Annual Forum Proceedings*, Fort Worth, Texas, May 2017.

10. Point of Contact in Navy

Marshall S. Hynes
Naval Air Systems Command Code 4.3.2.4
Flight Dynamics
marshall.hynes@navy.mil
301-342-8552 (Voice)

11. Acknowledgement/Disclaimer

This work was sponsored by the Office of Naval Research, ONR, under grant/contract number N00014-14-C-0004. The views and conclusions contained herein are those of the authors and should not be interpreted as necessarily representing the official policies or endorsements, either expressed or implied, of the Office of Naval Research, or the U.S. government.

Formatted: Justified, No widow/orphan control, Don't hyphenate, Font Alignment: Baseline

Section II: Project Metrics

Contract # N00014-14-C-0004

Autonomous Control Modes and Optimized Path Guidance for Shipboard Landing in High Sea States

Progress Report (CDRL A002)

Progress Report for Period: January 10, 2016 to April 9, 2017

PI: Joseph F. Horn 814-865-6434 joehorn@psu.edu Junfeng Yang Grad. Research Assistant Penn State University	Co-PI: Chengjian He (408) 523-5100 he@flightlab.com Dooyong Lee Advanced Rotorcraft Technologies	Co-PI: Marshall S. Hynes 301-342-8552 marshall.hynes@navy.mil Geraldo Gonzalez NAVAIR 4.3.2.4 John Tritschler U.S. Navy Test Pilot School

April 25, 2017

1. Metrics

Number of faculty supported under this project during this reporting period: 1

Number of post-doctoral researchers supported under this project during this period: 0

Number of graduate students supported under this project during this reporting period: 1

Number of undergraduate students supported under this project during this period: 0

Number of refereed publications during this reporting period for which at least 1/3 of the work was done under this effort: 0

Number of publications (all) during this reporting period: 1

Number of patents during this reporting period: 0

Number of M.S. students graduated during this reporting period: 0

Number of Ph.D. students graduated during this reporting period: 0

Awards received during this reporting period: 0

Invited talks given: 0

Conferences at which presentations were given (not including invited talks above): 1